Int. J. Heat Mass Transfer. Vol. 28, No. 1, pp. 253–264, 1985
Printed in Great Britain

0017-9310/85 $3.00 + 0.00

Laminar forced convection from a rotating cylinder

H. M. BADR
Mechanical Engineering Department, University of Petroleum & Minerals, Dhahran, Saudi Arabia

and

S. C. R. DENNIS
Applied Mathematics Department, University of Western Ontario, London, Canada

(*Received* 27 *September* 1983 *and in revised form* 19 *June* 1984)

Abstract—The problem of laminar forced convective heat transfer from an isothermal circular cylinder rotating about its own axis and placed in a uniform stream is considered. The direction of the forced flow of the cooling fluid is assumed to be normal to the cylinder axis. The study is based on the solution of the unsteady two-dimensional conservation equations of mass, momentum and energy. The problem is solved for Reynolds number (based on the free stream velocity) up to $Re = 100$ and for velocity ratios (ratio between cylinder circumferential velocity and free stream velocity) up to $\alpha = 4$. Major emphasis is given to the effect of the speed of rotation on the thermal boundary layer geometry and also on the local Nusselt number distribution.

INTRODUCTION

HEAT transfer from rotating bodies is one of the important problems that is receiving growing attention due to its engineering applications, such as heat transfer from rotating machinery, spinning projectiles and several others. According to the literature, the available information in this area is rather limited to a few special cases. A general method for solving such problems is not easily available, not only due to the mathematical difficulties involved but also due to the wide range of body shapes as well as the different characteristics of the velocity and thermal fields.

Experimental and theoretical investigations were previously conducted to evaluate the effect of rotation on the rate of heat transfer from spinning bodies. The velocity and temperature boundary layers over a rotating sphere in a forced convection heat transfer regime was studied by Siekmann [1] who obtained a solution to the boundary layer equations using the Blasius series method. The solution is limited to the case when the free stream velocity is parallel to the axis of rotation of the sphere and is valid up to the point of separation but not after. A method for the calculation of the heat transfer rate from rotating axisymmetric bodies in a laminar forced convection regime was given by Lee *et al.* [2]. The method, which is based on a series solution of the boundary layer and energy equations, is limited to cases in which the free stream velocity is parallel to the axis of symmetry. The same problem was investigated by Jeng *et al.* [3], however, for the special case when the body surface has a step discontinuity in its temperature. Heat transfer from axisymmetric rotating bodies flying at supersonic speeds was studied by Chou and Kalina [4] who found that increasing the speed of rotation tends to decrease the local Nusselt number over all the body surface except for a small region in the neighborhood of the stagnation point.

Convective heat transfer from an isothermal axisymmetric body rotating in a fluid at rest was investigated by Dorfman and Serazetdinov [5]. The investigation was limited to laminar boundary layer flows when the buoyant forces are negligibly small. Although the approach was tailored for exponentially shaped bodies, it was extended to obtain approximate solutions for spinning bodies having other shapes. The same problem was reinvestigated by Dorfman and Selyavin [6], however, for the general case of arbitrary surface temperature distribution. The turbulent heat transfer from a circular cylinder rotating in a motionless fluid was studied by Sherstyuk [7] in which a mathematical model was presented for the friction factor as well as the heat transfer coefficient. The same problem studied in [5] was later considered by Suwono [8] where a series solution method was adopted for solving the velocity and thermal boundary layer equations.

Experimental investigation of the effect of rotation on heat transfer rates from a horizontal cylinder spinning around its own axis in a quiescent fluid were conducted by Anderson and Saunders [9], Etemad [10], Dropkin and Carmi [11] and Becker [12]. A theoretical study of the same problem at low rotational speeds is found in the work by Goettler and Fillo [13]. The study was based on a series solution of the governing equations of motion and energy. A comparison between the experimental and theoretically deduced isotherms shows some considerable differences.

Relatively few studies have been carried out on the problem of convective heat transfer from a rotating cylinder in a cross-stream. Among these studies is the experimental work by Kays and Biorklund [14] who found that the heat transfer regime is dominated by the cross-flow for speed ratios (ratio between cylinder peripheral velocity and the free stream velocity) up to 2.

NOMENCLATURE

a	cylinder radius
c	specific heat
F_0, f_n, F_n	functions defined in equation (6)
G_0, g_n, G_n	functions defined in equation (6)
$h, \bar{h}$	local and average heat transfer coefficients
H_0, h_n, H_n	functions defined in equation (6)
k	thermal conductivity
$Nu, \overline{Nu}$	local and average Nusselt numbers
Pe	Peclet number
Pr	Prandtl number
r	radial coordinate
Re	Reynolds number, $2au_\infty/\nu$
T	temperature
u_∞	free stream velocitv
v_r, v_θ	radial and transverse components of velocity.

Greek symbols

α	speed radio, $a\omega/u_\infty$
δ	constant defined following equation (10)
ξ	dimensionless logarithmic radial coordinate, $\ln(r/a)$
μ	dynamic viscosity
ν	kinematic viscosity
ϕ	dimensionless temperature, $(T-T_\infty)/(T_s-T_\infty)$
ψ	dimensionless stream function, ψ'/au_∞
θ	angular coordinate
τ	normalized time, $\tau' u_\infty/a$
ω	angular velocity of cylinder
ζ	dimensionless vorticity, $a\zeta'/u_\infty$.

At higher speed ratios the heat transfer process becomes dominated by the rotational flow motion. A correlation was given for the heat transfer coefficient taking into account the combined effect of rotation, free convection and cross-flow. A theoretical study for the same problem, but limited to forced convection, was carried out by Vasilev and Golubev [15]. However, the study was based on a potential flow solution to simulate the velocity field around the cylinder. It seems from the literature that an accurate theoretical analysis to the problem of convective heat transfer from a rotating cylindrical body in a cross-stream is not available. The difficulty in tackling this problem arises from the lack of information about the actual boundary layer characteristics near the rotating body. For such problems the velocity field depends on the body geometry, fluid properties, free stream velocity, speed of rotation as well as the ratio between the buoyant and inertial forces.

In this work, the problem of forced convective heat transfer from a circular cylinder rotating around its own axis and placed in a uniform stream of a cooling fluid is considered. The free stream velocity is assumed to be normal to the cylinder axis while the cylinder surface temperature is assumed uniform. The most emphasis is given to the effect of rotation on the convective heat transfer process. The analysis is based on the solution of the full conservation equations of mass, momentum and energy for the case of a two-dimensional laminar forced convection regime.

GOVERNING EQUATIONS AND METHOD OF SOLUTION

Consider the problem of two-dimensional incompressible flow of a viscous cooling fluid over a hot circular cylinder of radius a, rotating around its own fixed axis with an angular velocity ω. The free stream of the cooling fluid, which is assumed to be uniform, is directed normal to the cylinder axis and has a uniform temperature T_∞. The cylinder surface is isothermal with a constant temperature T_s. The temperature difference between the main flow and the cylinder surface $\Delta T(=T_s-T_\infty)$ is assumed so small that the buoyant forces are negligible in comparison with the inertial forces. Accordingly, the fluid properties are considered the same through the entire flow field. The polar coordinate system (r, θ) is defined such that the free stream direction is $\theta = 0$. By introducing the modified system (ξ, θ) where $\xi = \ln(r/a)$, the governing equations of mass, momentum and energy can be expressed in the form of the vorticity, stream function and energy equations as

$$e^{2\xi}\frac{\partial \zeta}{\partial \tau} = -\frac{\partial \psi}{\partial \theta}\frac{\partial \zeta}{\partial \xi} + \frac{\partial \psi}{\partial \xi}\frac{\partial \zeta}{\partial \theta} + \frac{2}{Re}\left(\frac{\partial^2 \zeta}{\partial \xi^2} + \frac{\partial^2 \zeta}{\partial \theta^2}\right) \tag{1}$$

$$e^{2\xi}\zeta = \frac{\partial^2 \psi}{\partial \xi^2} + \frac{\partial^2 \psi}{\partial \theta^2} \tag{2}$$

$$e^{2\xi}\frac{\partial \phi}{\partial \tau} = -\frac{\partial \psi}{\partial \theta}\frac{\partial \phi}{\partial \xi} + \frac{\partial \psi}{\partial \xi}\frac{\partial \phi}{\partial \theta} + \frac{2}{Pe}\left(\frac{\partial^2 \phi}{\partial \xi^2} + \frac{\partial^2 \phi}{\partial \theta^2}\right) \tag{3}$$

where the dimensionless quantities $\tau, \zeta, \psi, \phi, Re$ and Pe are defined as $\tau = \tau' u_\infty/a$, $\zeta = \zeta' a/u_\infty$, $\psi = \psi'/au_\infty$, $\phi = (T-T_\infty)/(T_s-T_\infty)$, $Re = 2au_\infty/\nu$ and $Pe = Re\,Pr$, where Re is the Reynolds number, ν is the kinematic viscosity, Pe is the Peclet number and Pr is the Prandtl number. All quantities with primes are dimensional quantities.

The radial and transverse velocity components v_r and v_θ are defined as

$$v_r = v_r'/u_\infty = e^{-\xi}\,\partial\psi/\partial\theta$$
$$v_\theta = v_\theta'/u_\infty = -e^{-\xi}\,\partial\psi/\partial\xi. \tag{4}$$

The no-slip, impermeability and isothermal conditions at the cylinder surface can be expressed as

$$\psi = \partial\psi/\partial\theta = 0, \quad \partial\psi/\partial\xi = -\alpha$$

and (5a)

$$\phi = 1 \quad \text{at} \quad \xi = 0$$

while the free stream conditions far away from the cylinder can be represented by

$$\begin{aligned} &e^{-\xi}\,\partial\psi/\partial\theta \to \cos\theta, \quad e^{-\xi}\,\partial\psi/\partial\xi \to \sin\theta \\ &\zeta \to 0 \quad \text{and} \quad \phi \to 0 \quad \text{as} \quad \xi \to \infty \end{aligned} \tag{5b}$$

where α ($= a\omega/u_\infty$) is the ratio between the cylinder circumferential velocity and the free stream velocity.

The method used for solving equations (1)–(3) in order to obtain the details of the steady (or quasisteady) flow and thermal fields is based on studying the time evolution of the two fields until steady conditions are achieved. In the method, the fluid motion is assumed to start impulsively from rest and at the same time the cylinder starts its rotational motion with constant angular velocity ω. With no temperature difference present between the cylinder surface and the main stream, the velocity boundary layer starts to grow with time. Later on, when the boundary layer thickens, the cylinder surface is assumed to be suddenly heated to the constant temperature T_s. This step increase in temperature is followed by the simultaneous time development of the velocity and temperature boundary layers until reaching the steady (or quasisteady) conditions. The approach is, in principle, similar to that used by Dennis and Staniforth [16], Patel [17], Badr and Dennis [18] and by Badr [19]. In this approach we express the vorticity, stream function and temperature asymmetric fields in terms of Fourier series expansions as

$$\zeta(\xi,\theta,\tau) = \tfrac{1}{2}G_0(\xi,\tau) + \sum_{n=1}^{N} [g_n(\xi,\tau)\sin n\theta + G_n(\xi,\tau)\cos n\theta] \tag{6a}$$

$$\psi(\xi,\theta,\tau) = \tfrac{1}{2}F_0(\xi,\tau) + \sum_{n=1}^{N} [f_n(\xi,\tau)\sin n\theta + F_n(\xi,\tau)\cos n\theta] \tag{6b}$$

$$\phi(\xi,\theta,\tau) = \tfrac{1}{2}H_0(\xi,\tau) + \sum_{n=1}^{N} [h_n(\xi,\tau)\sin n\theta + H_n(\xi,\tau)\cos n\theta]. \tag{6c}$$

Substituting from equation (6) into equations (1)–(3) results in the following three sets of differential equations:

$$e^{2\xi}\frac{\partial G_0}{\partial \tau} = \frac{2}{Re}\frac{\partial^2 G_0}{\partial \xi^2} + S_0 \tag{7a}$$

$$2e^{2\xi}\frac{\partial g_n}{\partial \tau} = \frac{4}{Re}\left(\frac{\partial^2 g_n}{\partial \xi^2} - n^2 g_n\right) + nF_n\frac{\partial G_0}{\partial \xi} - nG_n\frac{\partial F_0}{\partial \xi} + S_{n_1} \tag{7b}$$

$$2e^{2\xi}\frac{\partial G_n}{\partial \tau} = \frac{4}{Re}\left(\frac{\partial^2 G_n}{\partial \xi^2} - n^2 G_n\right) - nf_n\frac{\partial G_0}{\partial \xi} - ng_n\frac{\partial F_0}{\partial \xi} + S_{n_2} \tag{7c}$$

$$\frac{\partial^2 F_0}{\partial \xi^2} = e^{2\xi} G_0 \tag{8a}$$

$$\frac{\partial^2 f_n}{\partial \xi^2} - n^2 f_n = e^{2\xi} g_n \tag{8b}$$

$$\frac{\partial^2 F_n}{\partial \xi^2} - n^2 F_n = e^{2\xi} G_n \tag{8c}$$

$$e^{2\xi}\frac{\partial H_0}{\partial \tau} = \frac{2}{Pe}\frac{\partial^2 H_0}{\partial \xi^2} + Y_0 \tag{9a}$$

$$2e^{2\xi}\frac{\partial h_n}{\partial \tau} = \frac{4}{Pe}\left(\frac{\partial^2 h_n}{\partial \xi^2} - n^2 h_n\right) + nF_n\frac{\partial H_0}{\partial \xi} - nH_n\frac{\partial F_0}{\partial \xi} + Y_{n_1} \tag{9b}$$

$$2e^{2\xi}\frac{\partial H_n}{\partial \tau} = \frac{4}{Pe}\left(\frac{\partial^2 H_n}{\partial \xi^2} - n^2 H_n\right) - nf_n\frac{\partial H_0}{\partial \xi} + nh_n\frac{\partial F_0}{\partial \xi} + Y_{n_2} \tag{9c}$$

where $F_0 = F_0(\xi,\tau)$, $G_0 = G_0(\xi,\tau), \ldots$, etc. and S_0, S_{n_1}, S_{n_2}, Y_0, Y_{n_1} and Y_{n_2} are functions of ξ and τ and are all defined in the Appendix. The boundary conditions for the functions given in equations (7)–(9) are obtained from equations (5) and (6) and can be expressed as

$$\begin{aligned} &F_0 = f_n = F_n = h_n = H_n = 0 \\ &\partial f_n/\partial\xi = \partial F_n/\partial\xi = 0, \quad \partial F_0/\partial\xi = -2\alpha, \\ &H_0 = 2 \text{ at } \xi = 0 \end{aligned} \tag{10a}$$

$$\begin{aligned} &F_n, G_0, g_n, H_0, h_n \quad \text{and} \quad H_n \to 0 \\ &f_n \to e^{\xi}\delta_n, \quad \partial F_0/\partial\xi \to 0 \quad \text{as} \quad \xi \to \infty \end{aligned} \tag{10b}$$

where $\delta_n = 1$ for $n = 1$ and $\delta_n = 0$ for $n \neq 1$. Also, by integrating both sides of each of equations (8a)–(8c) with respect to ξ between the limits 0 and ∞, and using the boundary conditions given in equation (10) we obtain the following integral conditions

$$\int_0^\infty e^{2\xi} G_0(\xi,\tau)\,d\xi = 2\alpha \tag{11a}$$

$$\int_0^\infty e^{(2-n)\xi} G_n(\xi,\tau)\,d\xi = 0 \tag{11b}$$

$$\int_0^\infty e^{(2-n)\xi} g_n(\xi,\tau)\,d\xi = 2\delta_n. \tag{11c}$$

The above integral conditions are used for calculating the values of the functions G_0, G_n and g_n on the cylinder surface ($\xi = 0$) at each time step for better accuracy. Condition (11a) is also important to ensure the continuity of pressure around the cylinder surface.

The time required for the evolution of the velocity and thermal boundary layers has been divided into two distinct periods. The first period begins when the free stream and the cylinder start their impulsive motions from rest. Analytical solutions for the stream function and vorticity at $\tau = 0$ were previously obtained [18] and used as initial conditions in the numerical solution. Because of the small boundary layer thickness prevailing in this period the logarithmic coordinate ξ was replaced by the boundary layer coordinate x such that $\xi = 2(2\tau/Re)^{1/2}x$ following references [18] and [20]. The numerical technique used for solving equations (7) and (8) to advance the solution of ψ and ζ in time is exactly the same as that used in [18] and [19]. The numerical integration in this period is terminated at time $\tau = Re/8$ at which the boundary layer becomes thick enough for utilizing the original coordinate ξ.

The second period starts following the end of the first one where the full details of the velocity field are known. The cylinder surface temperature is now assumed to be instantaneously raised to T_s. According to the previous assumptions, the temperature rise will have no effect on the time development of the velocity field since the buoyant forces are assumed negligible. The three sets of differential equations are now integrated simultaneously in order to advance the solution of ψ, ζ and ϕ in time until reaching steady state when there is no vortex shedding or a quasisteady condition when vortex shedding takes place.

Following reference [19] the number of terms N in the Fourier series was 2 at the start of the first period. This number was allowed to increase with time whenever any of the last non-zero terms in the series reaches a certain small value ($\simeq 10^{-4}$). However, the maximum number of terms used in all cases was 20. During the first period of motion a step size $\Delta x = 0.05$ was used while 161 points were utilized in the x direction. On the other hand, the step size $\Delta\xi$ during the second period was 0.1. The number of points in ξ and accordingly the size of the flow domain were changing with time in order to minimize the time of computation. The outer boundary of the flow domain is determined such that the values of ζ and ϕ at that boundary are below a certain small limit ($\simeq 10^{-10}$). The maximum value of ξ used in all cases was 10 which corresponds to a distance away from the cylinder as far as e^{10} times its radius. The details of the numerical method are as given in reference [19].

DISCUSSION OF RESULTS

The influence of the cylinder rotation on the thermal boundary layer characteristics and on the overall heat transfer rate is investigated in the range of Reynolds numbers from $Re = 5$ to $Re = 100$, and in the range of speed ratios from $\alpha = 0.1$–4. Let us now define the local and average Nusselt numbers as

$$Nu = 2ah/k \quad \text{and} \quad \overline{Nu} = 2a\bar{h}/k \tag{12}$$

where k is the coefficient of thermal conductivity of the fluid and h and $\bar{h}$ are the local and average heat transfer coefficients which are related to the temperature field by

$$h = -k(\partial T/\partial r)_{r=a}/(T_s - T_\infty), \quad \bar{h} = (1/2\pi)\int_0^{2\pi} h\, d\theta. \tag{13}$$

The relationship between each of Nu and $\overline{Nu}$ and the functions H_0, h_n, H_n can be easily deduced from equations (6), (12) and (13) and can be written as

$$Nu = \left[-\partial H_0/\partial\xi - 2\sum_{n=1}^{N} \{\partial h_n/\partial\xi \sin n\theta + \partial H_n/\partial\xi \cos n\theta\} \right]_{\xi=0} \tag{14a}$$

$$\overline{Nu} = [-\partial H_0/\partial\xi]_{\xi=0}. \tag{14b}$$

The results obtained showed that the local Nusselt number, as well as the surface vorticity distributions, are highly influenced by the rotational motion of the cylinder. Figure 1(a) shows the distribution of Nu around the cylinder surface for the case of $Re = 5$ and different rotational speeds. At low values of α ($\alpha = 0.1$) the variation of Nu deviates only slightly from the symmetrical distribution around the line $\theta = 0$ (or $\theta = 180°$) that prevails in the case of a fixed cylinder. One can also see from Fig. 1(a) that the curve showing the variation of Nu tends to flatten as the rotational speed

Table 1. Values of the average Nusselt number at different Reynolds numbers and speed ratios

Re	α	$\overline{Nu}$
5	0.1	1.440
	0.5	1.437
	1.0	1.431
	2.0	1.407
	4.0	1.355
20	0.1	2.512
	0.5	2.509
	1.0	2.473
	2.0	2.364
	4.0	2.203
40	0.1	3.508
	0.5	3.471
	1.0	3.405
	2.0	3.141
	4.0	2.760
60	0.1	4.105
	0.5	4.101
	1.0	4.026
	2.0	3.682
	4.0	3.055
100	0.1	5.364
	0.5	5.311
	1.0	5.139
	2.0	4.546
	4.0	3.413

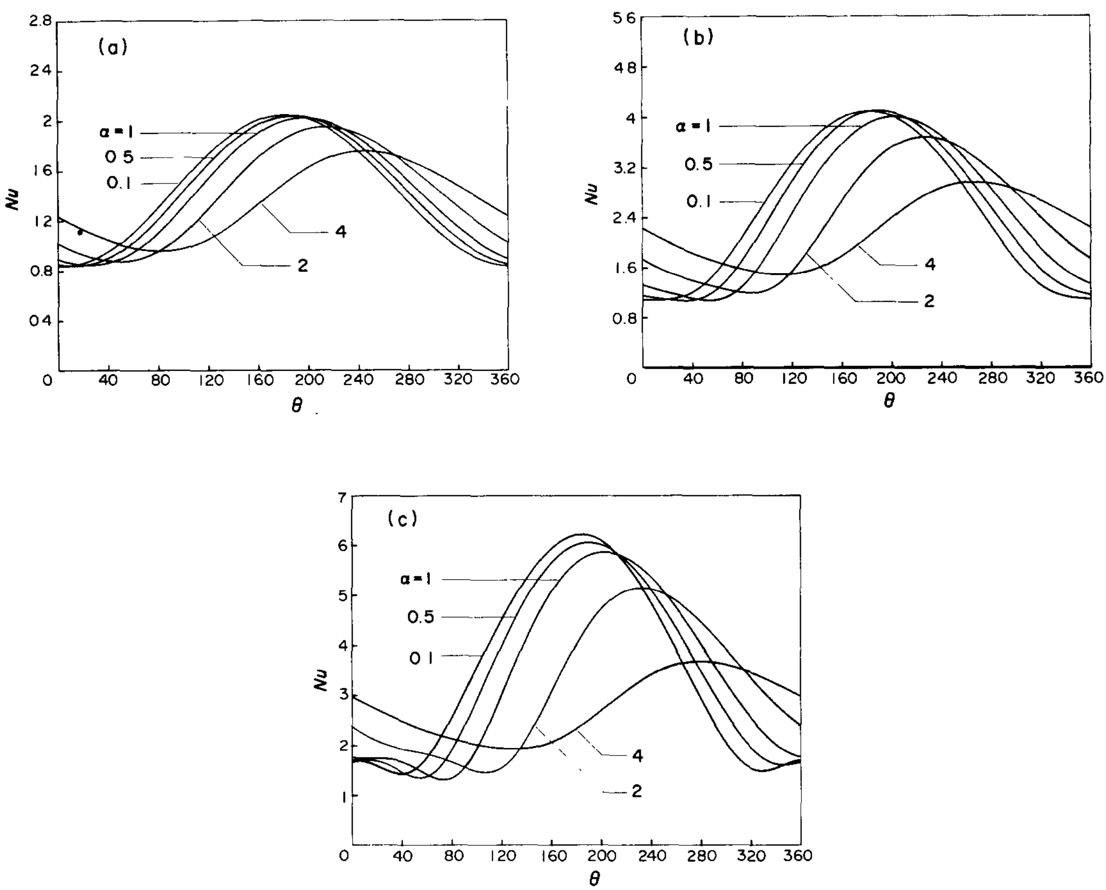

FIG. 1. The effect of the speed ratio on the local Nusselt number distribution around the cylinder surface for the case of $Pr = 0.7$ and (a) $Re = 5$, (b) $Re = 20$ and (c) $Re = 40$.

increases. The same phenomenon occurred at higher values of Reynolds number as can be seen in Fig. 1(b) and 1(c). This behavior is expected since as α increases the flow region surrounding the cylinder becomes more dominated by the speed of rotation and not by the main flow velocity. A similar behavior, but for the heat transfer coefficient, was found experimentally by Kays and Biorklund [14] although their work was carried out at much higher values of Reynolds numbers.

The effect of rotation on the location of the points of maximum and minimum local heat transfer coefficients can also be seen in Fig. 1 where both points are shifted in the same direction of the cylinder rotation. For example, in the case of $Re = 5$, the point of maximum Nusselt number has been shifted from $\theta = 180°$ to $\theta \simeq 246°$ at $\alpha = 4$, while the point of minimum Nusselt number has been shifted from $\theta = 0$ to $\theta \simeq 82°$. The effect of rotation on the vorticity distribution on the cylinder surface can be seen in Fig. 2(a)–(c) for Reynolds numbers of $Re = 5$, 20 and 40, respectively. At higher Re values ($Re = 60$ and 100) the velocity field ceases to be steady due to vortex shedding except at high rotational speeds. Accordingly, the local Nusselt number and vorticity distributions given in Fig. 3(a) and (b) for the case of $Re = 60$ are only plotted at a certain selected time. These curves are periodically changing in accordance with the velocity and temperature fields.

The calculated values of the average Nusselt number at different Reynolds numbers and rotational speeds are listed in Table 1. The table shows that $\overline{Nu}$ decreases as α increases in the considered range of Re and α. This behavior is similar to the findings of Chou and Kalina [4] for the case of high speed flow over an axisymmetric rotating body. The phenomenon can be explained on the basis that due to the rotational motion of the cylinder it becomes surrounded with a certain volume of rotating fluid that never gets entrained to the main stream. This rotating fluid acts as a buffer zone between the cylinder and the free stream. Such flow field characteristics will restrict the heat transfer regime between the rotating fluid and the main stream to conduction only. This effect will naturally tend to decrease the overall heat transfer rate. It should be mentioned here that the values obtained of the average Nusselt number at small speed ratios ($\alpha = 0.1$) are found to differ only slightly from the values obtained for a fixed cylinder by Dennis *et al.* [21] and by Hatton *et al.* [22]. This also serves as a check to the accuracy of the method of solution.

To show the effect of rotation on the velocity and thermal fields the streamline and isotherm patterns are

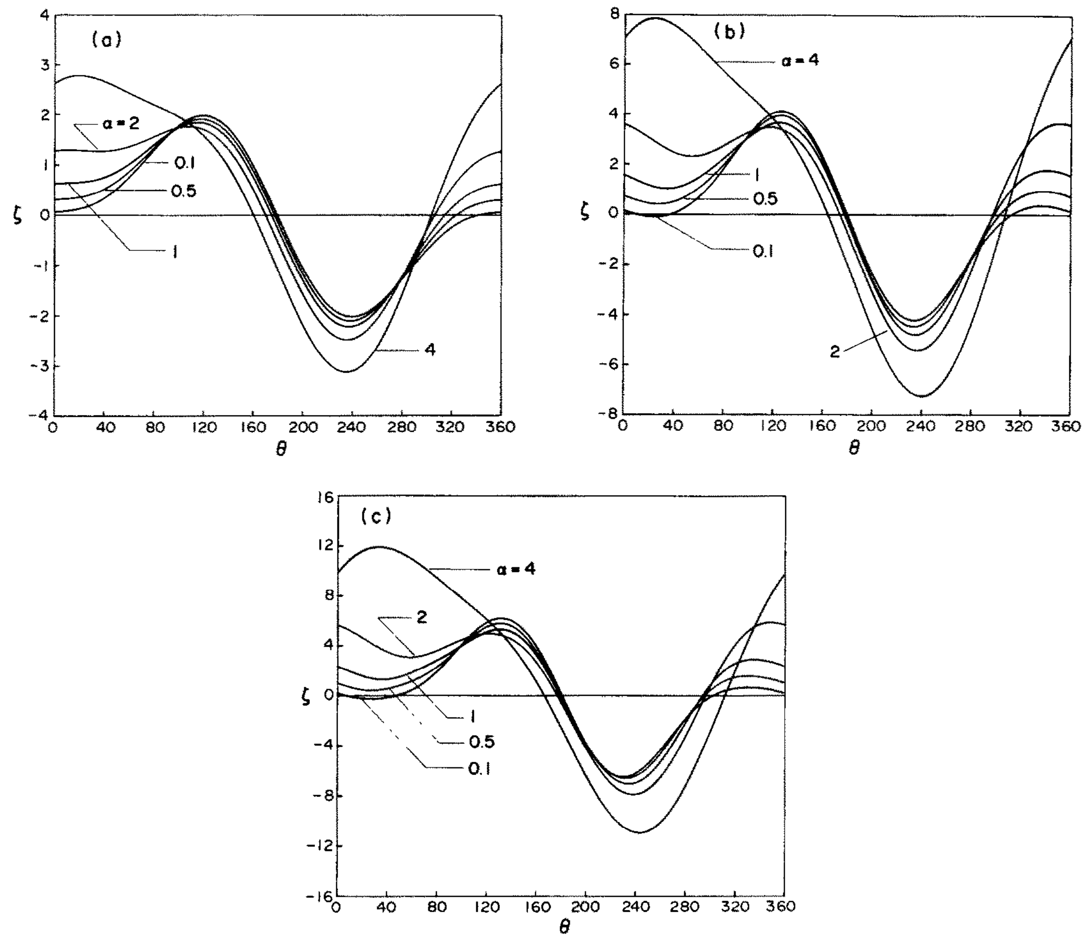

FIG. 2. The effect of the speed ratio on the surface vorticity distribution for the case of (a) $Re = 5$, (b) $Re = 20$ and (c) $Re = 40$.

plotted in Figs 4–6 for the cases of $Re = 5, 20$ and 40 at different speed ratios. One can see from Figs 4(b), 5(b) and 6(b) that increasing α tends to increase the volume of the isolated fluid rotating around the cylinder. It can also be seen that the circulating fluid zone in the wake of the cylinder completely disappears at high speeds of rotation. The isotherm patterns for the cases of $Re = 5, 20$ and 40 show the strong dependence of the temperature field on the rotational motion of the cylinder. At small values of α ($\alpha = 0.1$) the isotherms are almost symmetrical around the line $\theta = 0$. It can also be seen that as α increases all the isotherms are found to be

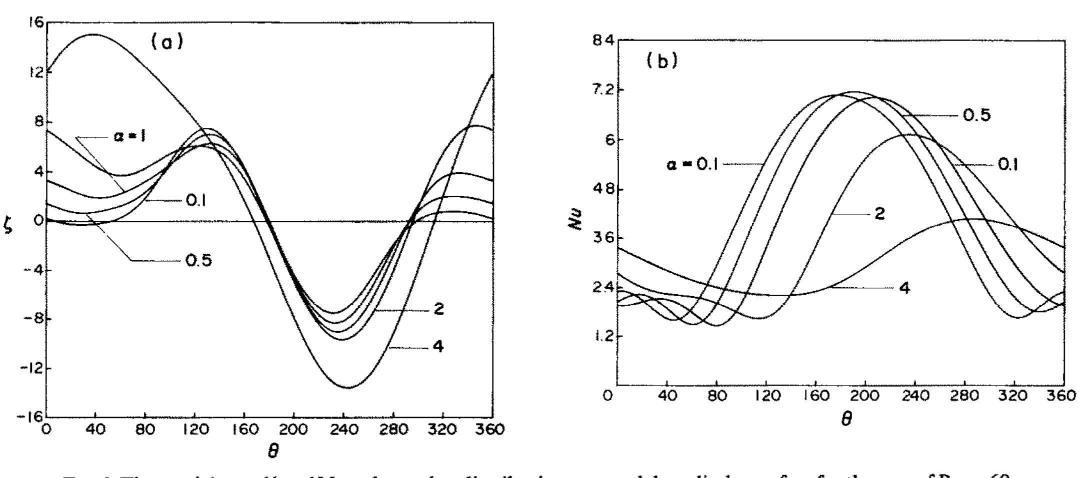

FIG. 3. The vorticity and local Nusselt number distributions around the cylinder surface for the case of $Re = 60$, $Pr = 0.7$ at $\tau = 20$; (a) vorticity, and (b) local Nusselt number.

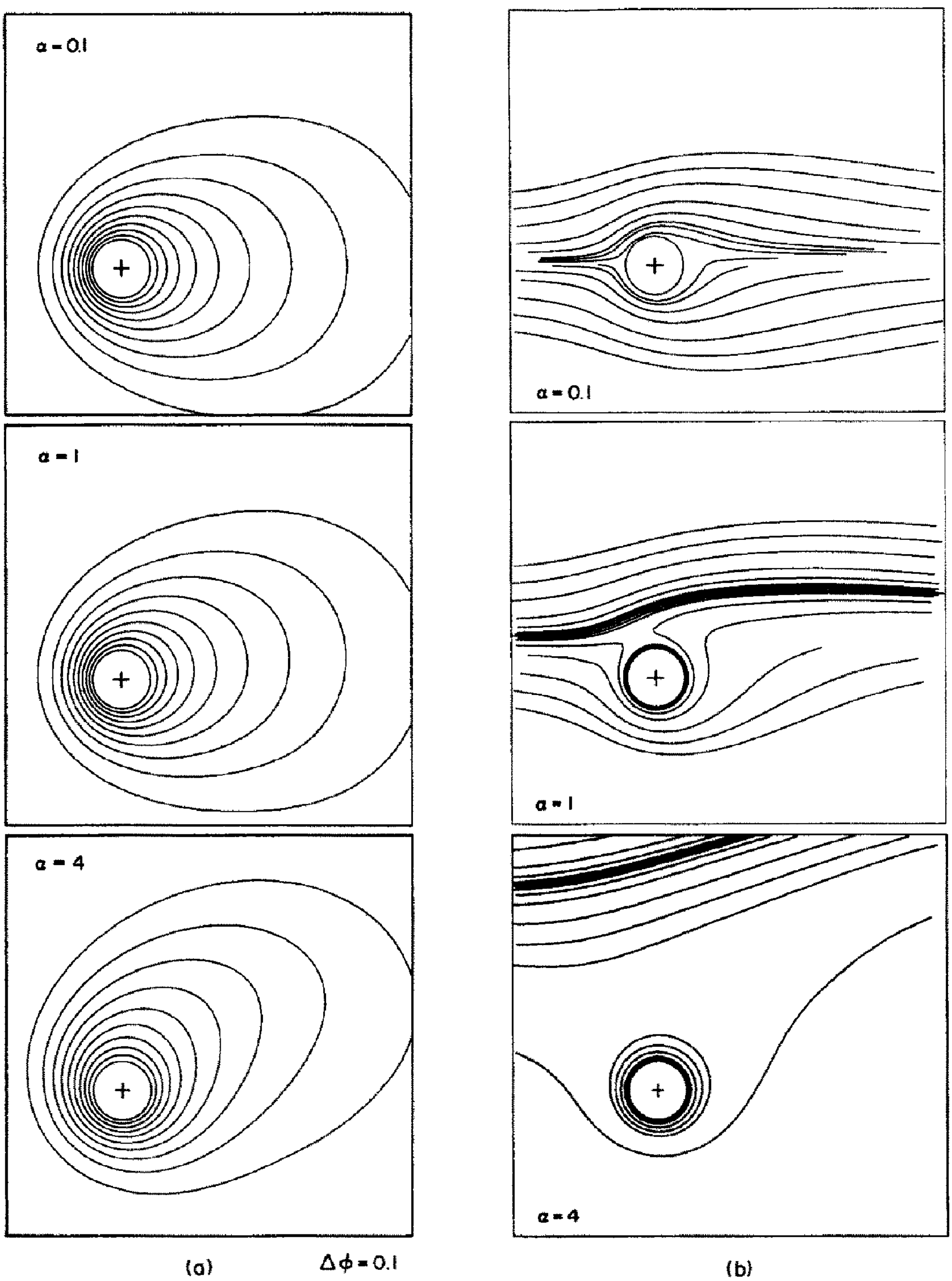

Fig. 4. The isotherm and streamline patterns for the case of $Re = 5$ and $Pr = 0.7$ at different speed ratios, (a) isotherms, (b) streamlines.

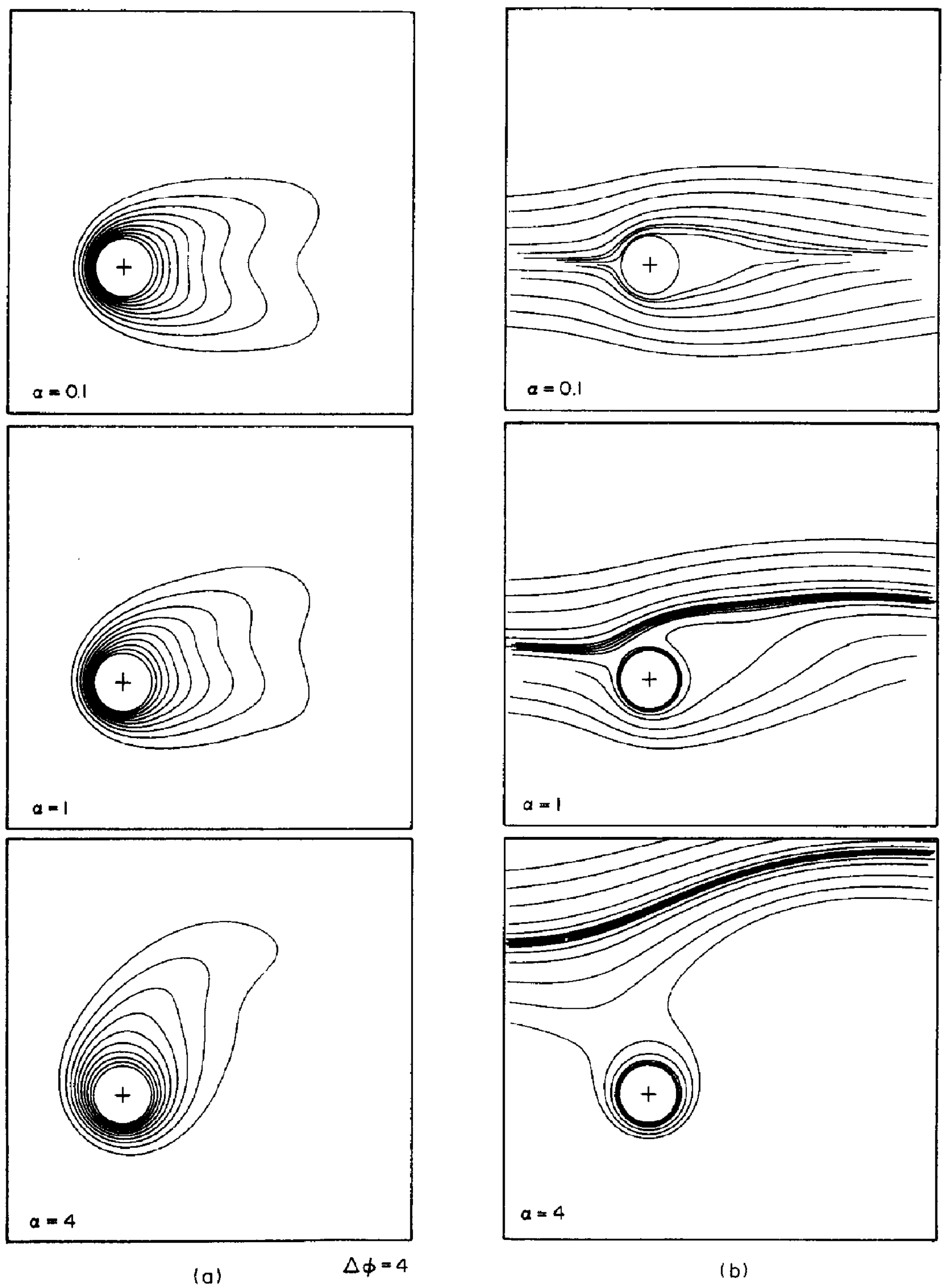

FIG. 5. The isotherm and streamline patterns for the case of $Re = 20$ and $Pr = 0.7$ at different speed ratios, (a) isotherms, (b) streamlines.

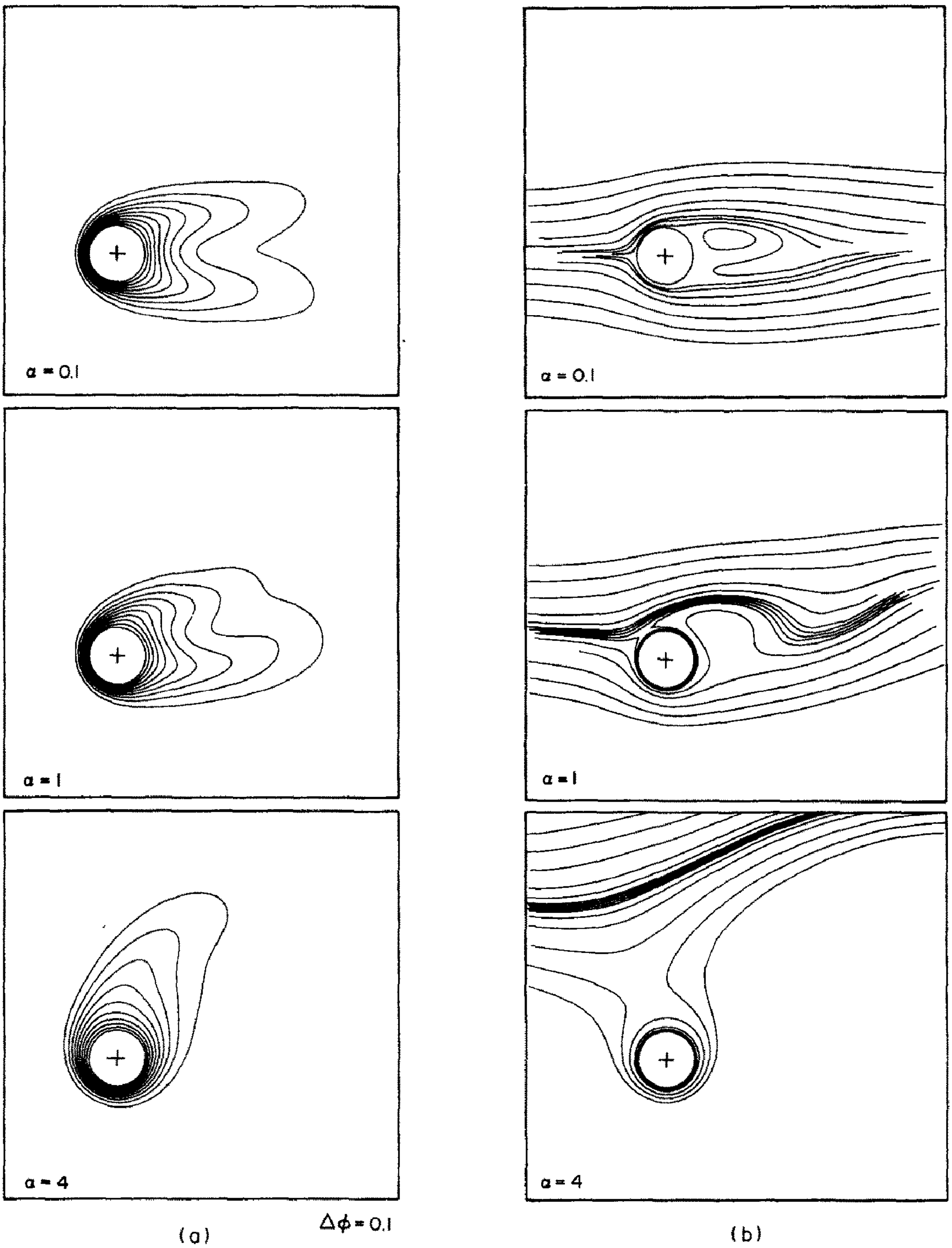

FIG. 6. The isotherm and streamline patterns for the case of $Re = 40$, $Pr = 0.7$ at different speed ratios, (a) isotherms, (b) streamlines.

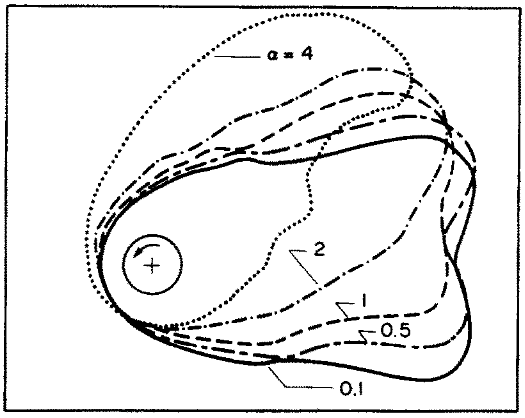

Fig. 7. The effect of rotation on the thermal boundary layer thickness around the cylinder for the case of $Re = 40$.

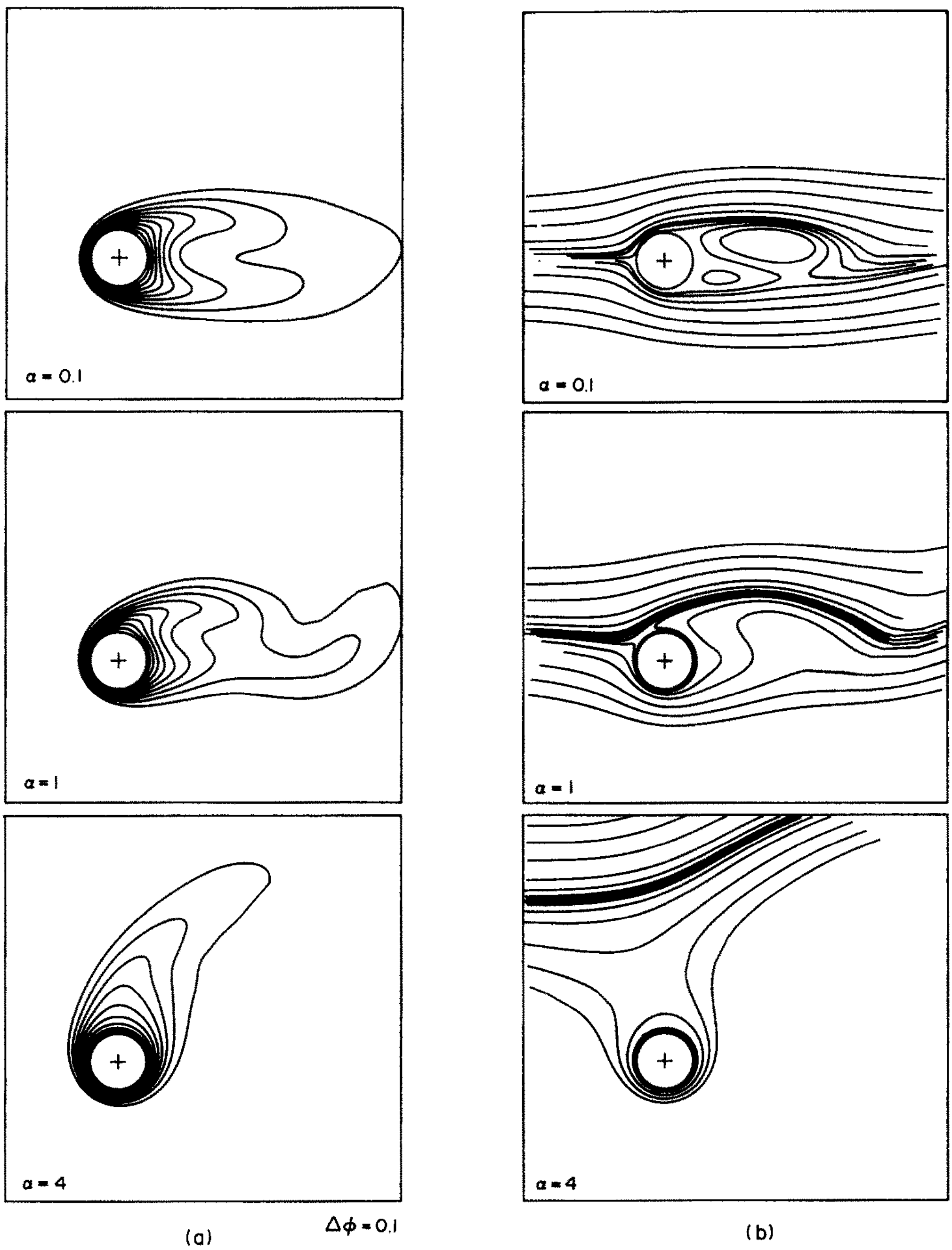

Fig. 8. The isotherm and streamline patterns for the case of $Re = 60$, $Pr = 0.7$ at different speed ratios and at $\tau = 20$, (a) isotherms, (b) streamlines.

displaced upward and the points of maximum and minimum temperature gradients are shifted as shown in Fig. 1. If one considers the edge of the thermal zone bounding the cylinder to exist at $\phi = 0.01$, the effect of the rotational speed on its shape would be as shown in Fig. 7 for the case of $Re = 40$. The streamlines and isotherms are also plotted in Fig. 8 for the case of $Re = 60$ at a certain chosen time. However, since there is no steady state at small values of α the velocity and thermal fields continue to change periodically.

CONCLUSION

The effect of rotational motion on forced convective heat transfer from a circular cylinder is studied in the range of Reynolds numbers up to 100 and speed ratios up to 4. In the considered range, it is found that the flow and thermal fields are strongly influenced by the speed of rotation of the cylinder. The overall heat transfer coefficient tends to decrease as the speed of rotation increases because of the existence of a rotating fluid layer that separates the cylinder from the main stream. The average values of the Nusselt number are listed for the different cases considered and the effect of rotational speed on the geometry of the thermal boundary layer is also investigated.

Acknowledgements—The authors wish to acknowledge the support received from the NSERC of Canada and the University of Petroleum & Minerals during the course of this study.

REFERENCES

1. J. Siekmann, The calculation of the thermal boundary layer on a rotating sphere, *Z. Angew Math. Phys.* **13**, 468–482 (1962).
2. M. H. Lee, D. R. Jeng and K. J. DeWitt, Laminar boundary layer transfer over rotating bodies in forced flow, *J. Heat Transfer* **100**, 496–502 (1978).
3. D. R. Jeng, K. J. DeWitt and M. H. Lee, Forced convection over rotating bodies with non-uniform surface temperature, *Int. J. Heat Mass Transfer* **22**, 89–98 (1979).
4. D. C. Chou and J. A. Kalina, Heat transfer characteristics and boundary layer development about heating and cooling rotating blunt bodies at supersonic speeds, *Proc. Seventh Int. Heat Transfer Conf.*, Munchen, FRG, Vol. 3, p. 143 (1982).
5. L. A. Dorfman and A. Z. Serazetdinov, Laminar flow and heat transfer near rotating axisymmetric surface, *Int. J. Heat Mass Transfer* **8**, 317–327 (1965).
6. A. S. Dorfman and G. F. Selyavin, Exact solution of equations of thermal boundary layer for axisymmetric rotating bodies with an arbitrary surface temperature distribution, *Heat Transfer-Soviet Res.* **9**, 105–113 (1977).
7. A. N. Sherstyuk, Friction factor and heat transfer coefficient of a rotating round cylinder, *Therm. Engng* **22**, 41–46 (1975).
8. A. Suwono, Heat transfer from rotating bodies of arbitrary contour, *J. Heat Transfer* **102**, 778–789 (1980).
9. J. T. Anderson and O. A. Saunders, Convection from an isolated heated horizontal cylinder rotating about its axis, *Proc. R. Soc. Lond. A* **217**, 555–562 (1953).
10. G. A. Etemad, Free convection heat transfer from a rotating horizontal cylinder to ambient air with interferometric study of flow, *Trans. Am. Soc. Mech. Engrs* **77**, 1283–1289 (1955).
11. D. Dropkin and A. Carmi, Natural convection heat transfer from a horizontal cylinder rotating in air, *Trans. Am. Soc. Mech. Engrs* **79**, 741–749 (1957).
12. K. M. Becker, Measurement of convective heat transfer from a horizontal cylinder rotating in a tank of water, *Int. J. Heat Mass Transfer* **6**, 1053–1062 (1963).
13. L. L. Goettler and J. A. Fillo, Free convection from a slowly rotating horizontal cylinder, *Proc. Fifth Int. Heat Transfer Conf.*, Tokyo, Japan, Vol. 3, pp. 207–211 (1974).
14. W. M. Kays and I. S. Biorklund, Heat transfer from a rotating cylinder with and without crossflow, *Trans. Am. Soc. Mech. Engrs* **80**, 70–78 (1958).
15. A. N. Vasilev and V. V. Golubev, Heat transfer from a rotating cylinder under forced convection, *Inzh.-Fiz. Zh.* **41**, 414–420 (1981).
16. S. C. R. Dennis and A. N. Staniforth, A numerical method for calculating the initial flow past a cylinder in a viscous fluid, *Proc. Second Int. Conf. Numerical Meth. Fluid Dynamics*, University of California, Berkeley, U.S.A., 15–19 September (1970).
17. V. A. Patel, Flow around the impulsively started elliptic cylinder at various angles of attack, *Computers Fluids* **9**, 435–462 (1981).
18. H. M. Badr and S. C. R. Dennis, Time-dependent flow past an impulsively started rotating and translating circular cylinder, *J. Fluid Mechanics* (in press) (1984).
19. H. M. Badr, A theoretical study of laminar mixed convection from a horizontal cylinder in a cross stream, *Int. J. Heat Mass Transfer* **26**, 639–653 (1983).
20. W. M. Collins and S. C. R. Dennis, Flow past an impulsively started circular cylinder, *J. Fluid Mech.* **60**, 105–127 (1973).
21. S. C. R. Dennis, J. D. Hudson and N. Smith, Steady laminar forced convection from a circular cylinder at low Reynolds number, *Physics Fluids* **11**, 933–940 (1967).
22. A. P. Hatton, D. D. James and H. W. Swire, Combined forced and natural convection with low speed air flow over horizontal cylinders, *J. Fluid Mech.* **42**, 17–31 (1970).

APPENDIX

The functions S_0, S_{n_1} and S_{n_2} given in equations (7a)–(7c) are defined as

$$S_0 = \sum_{n=1}^{N} n\left\{F_n\frac{\partial g_n}{\partial \xi} - f_n\frac{\partial G_n}{\partial \xi} + g_n\frac{\partial F_n}{\partial \xi} - G_n\frac{\partial f_n}{\partial \xi}\right\} \tag{A1}$$

$$\begin{aligned} S_{n_1} = \sum_{m=1}^{N} & \frac{\partial g_m}{\partial \xi}[Kf_K - Jf_J] + \frac{\partial G_m}{\partial \xi}[KF_K - (m-n)F_J] \\ & + mg_m\left[\frac{\partial f_K}{\partial \xi} - \operatorname{sgn}(m-n)\frac{\partial f_J}{\partial \xi}\right] + mG_m\left[\frac{\partial F_K}{\partial \xi} - \frac{\partial F_J}{\partial \xi}\right] \end{aligned} \tag{A2}$$

$$\begin{aligned} S_{n_2} = \sum_{m=1}^{N} & \frac{\partial g_m}{\partial \xi}[KF_K + (m-n)F_J] - \frac{\partial G_m}{\partial \xi}[Kf_k + Jf_J] \\ & + mg_m\left[\frac{\partial F_K}{\partial \xi} + \frac{\partial F_J}{\partial \xi}\right] - mG_m\left[\frac{\partial f_K}{\partial \xi} + \operatorname{sgn}(m-n)\frac{\partial f_J}{\partial \xi}\right] \end{aligned} \tag{A3}$$

where $K = m+n$, $J = |m-n|$, $\operatorname{sgn}(m-n)$ is the sign of the term $(m-n)$ and $\operatorname{sgn}(m-n) = 0$ when $m = n$. All the functions are equated to zero when their subscript exceeds N.

The functions Y_0, Y_{n_1} and Y_{n_2} written in equations (9a)–(9c) are defined as

$$Y_0 = \sum_{n=1}^{N} n\left(F_n\frac{\partial h_n}{\partial \xi} - f_n\frac{\partial H_n}{\partial \xi} + h_n\frac{\partial F_n}{\partial \xi} - H_n\frac{\partial f_n}{\partial \xi}\right) \tag{A4}$$

$$Y_{n_1} = \sum_{m=1}^{N} \frac{\partial h_m}{\partial \xi}[Kf_K - Jf_J] + \frac{\partial H_m}{\partial \xi}[Kf_K - (m-n)F_J] + mh_m\left[\frac{\partial f_K}{\partial \xi} - \mathrm{sgn}\,(m-n)\frac{\partial F_J}{\partial \xi}\right] + mH_m\left[\frac{\partial F_K}{\partial \xi} - \frac{\partial F_J}{\partial \xi}\right] \quad \text{(A5)}$$

$$Y_{n_2} = \sum_{m=1}^{N} \frac{\partial h_m}{\partial \xi}[KF_K + (m-n)F_J] - \frac{\partial H_m}{\partial \xi}[Kf_K + Jf_J] + mh_m\left[\frac{\partial F_K}{\partial \xi} + \frac{\partial F_J}{\partial \xi}\right] - mH_m\left[\frac{\partial f_K}{\partial \xi} + \mathrm{sgn}\,(m-n)\frac{\partial f_J}{\partial \xi}\right]. \quad \text{(A6)}$$

CONVECTION LAMINAIRE FORCEE AUTOUR D'UN CYLINDRE TOURNANT

Résumé—On considère le problème du transfert thermique par convection laminaire forcée autour d'un cylindre tournant autour de son axe et placé dans un courant uniforme. La direction de l'écoulement forcé du fluide refroidissant est normal à l'axe du cylindre. L'étude est basée sur la solution des équations de bilan, en régime variable bidimensionel, de masse, de quantité de mouvement et d'énergie. Le problème est résolu pour un nombre de Reynolds (basé sur la vitesse au loin) allant jusqu'à $Re = 100$ et pour des rapports de vitesse (rapport de la vitesse circonférentielle du cylindre à la vitesse du courant) allant jusqu'à $\alpha = 4$. Un intérêt particulier est porté à l'effet de la vitesse de rotation sur la géométrie de la couche limite thermique et aussi sur la distribution du nombre de Nusselt local.

LAMINARE ERZWUNGENE KONVEKTION AN EINEM ROTIERENDEN ZYLINDER

Zusammenfassung—Das Problem der Wärmeübertragung bei laminarer erzwungener Konvektion an einem isothermen kreisförmigen Zylinder wird betrachtet, welcher sich um seine eigene Achse dreht und sich in einer gleichförmigen, quergerichteten Strömung befindet. Die Untersuchung beruht auf der Lösung der instationären zweidimensionalen Erhaltungsgleichungen für Masse, Impuls und Energie. Das Problem wurde für Reynolds-Zahlen (gebildet mit der freien Strömungsgeschwindigkeit) bis zu $Re = 100$ und für Geschwindigkeitsverhältnisse (Verhältnis zwischen Zylinderumfangsgeschwindigkeit und freier Strömungsgeschwindigkeit) bis zu $\alpha = 4$ gelöst. Besondere Aufmerksamkeit wurde dem Einfluß der Rotationsgeschwindigkeit auf die Geometrie der thermischen Grenzschicht und auf die Verteilung der örtlichen Nusselt-Zahl verwandt.

ВЛИЯНИЕ ВРАЩЕНИЯ ЦИЛИНДРА НА КОНВЕКТИВНЫЙ ТЕПЛОПЕРЕНОС

Аннотация—Рассматривается задача о ламинарном вынужденном конвективном теплопереносе от изотермического круглого цилиндра, вращающегося вокруг собственной оси и помещенного в однородный поток жидкости. Предполагается, что вынужденный поток охлаждающей жидкости направлен перпендикулярно к оси цилиндра. Исследование проводится на основе решения нестационарных двумерных уравнений сохранения массы, импульса и энергии. Задача решается для значений числа Рейнольдса (вычисляемого по скорости невозмущенного потока) вплоть до $Re = 100$ и отношения скоростей (отношение окружной скорости цилиндра к скорости невозмущенного потока) вплоть до $\alpha = 4$. Основное внимание уделено исследованию влияния скорости вращения цилиндра на геометрию теплового пограничного слоя, а также на распределение локальных чисел Нуссельта.